IEEE Access
Multidisciplinary | Rapid Review | Open Access Journal

Received May 31, 2018, accepted June 29, 2018, date of publication July 10, 2018, date of current version August 15, 2018.

Digital Object Identifier 10.1109/ACCESS.2018.2852813

Exact Speed Tracking Realization of the Single Shaft Micro-Turbine System via Higher-Order Sliding Mode Observer

YUGE SUN[1], (Student Member, IEEE), CHUANLIN ZHANG[1], (Member, IEEE), HUI CHEN[1], (Member, IEEE), PENGFENG LIN[2,3], AND XINGCHEN XU[4], (Student Member, IEEE)

[1]School of Automation, Shanghai University of Electric Power, Shanghai 200090, China
[2]School of Interdisciplinary Graduate, Nanyang Technological University, Singapore 639798
[3]Energy Research Institute, Nanyang Technological University, Singapore 639798
[4]School of Automation, Huazhong University of Science and Technology, Wuhan 430074, China

Corresponding author: Hui Chen (chenhui@shiep.edu.cn)

This work was supported in part by the National Natural Science Foundation of China under Grant 61503236 and Grant 51705304, in part by the Shanghai Education Development Foundation and the Shanghai Municipal Education Commission through the Chenguang Program under Grant 15CG56, and in part by the Natural Science Foundation of Shanghai under Grant 16ZR1413400.

ABSTRACT We present in this paper, a composite control approach to realize the exact speed trajectory tracking for the single shaft micro-turbine (MT) system. The composite controller is developed by incorporating a higher-order sliding mode observer and a feedback domination technique. By mean of the proposed method, asymptotic stability of the MT system can be ensured even in the presence of mismatched disturbances. It is illustrated, by numerical simulations, how this handy machinery is feasible for the practical disturbed MT system to realize the exact tracking, rather than a practical tracking objective.

INDEX TERMS MT system, mismatched disturbance, higher-order sliding mode differentiator, non-recursive manner.

I. INTRODUCTION

Power industry has gradually changed its traditional structure, which paves the way to the new energy industry and promotes a significant growth of the role of Distributed Generation (DG) [1]. In recent years, Micro Turbine (MT) is extensively used as a DG source owing to its salient merits of high efficiency, fast starting speed and favorable peak shaving capacity [2]–[5].

The basic components of a single shaft MT generation system are a compressor, a combustor, a recuperator, a turbine, a Permanent Magnet Synchronous Generator (PMSG) and power electronic interfaces, as shown in Fig. 1. The working process of the MT, similar to the process of large gas turbines, can be concluded as a thermodynamic cycle. In this cycle, the inlet air is compressed into a compressor, and subsequently, a mixture of the compressed air and fuel burns in the combustor [6]. Then, the hyperthermal gas will be expanded through the turbine to produce the rotating mechanical power to drive the PMSG operating. The PMSG produces high frequency output voltage (in the order of kHz). This unsuitable power condition needs power electronic interfaces to change the frequency for general use [2]. Furthermore, LCL filter circuits are used to eliminate the harmonics produced by the power electronic switches. The MT system block is marked in Fig. 1.

In face of these complex components, many scholars try to establish a precise mathematical model to describe the real properties of the MT system. For example, in [7], a dynamic model of MT for grid/island operations is proposed. In [8], new dynamic MT models are built to well capture the interactions between natural gas networks and electric networks. In this paper, the popular and reliable Rowen's mathematical model proposed in [9] would be used and studied.

Regarding the high demand of the MT system control issue, numerous control strategies have been investigated in the literature. As a conventional fashion, the PID control strategy is widely used in the MT speed regulation [8], [10]. However, when it comes to a more complicated model with the presence of nonlinearities and uncertainties, the PID control performance possibly deteriorates and cannot

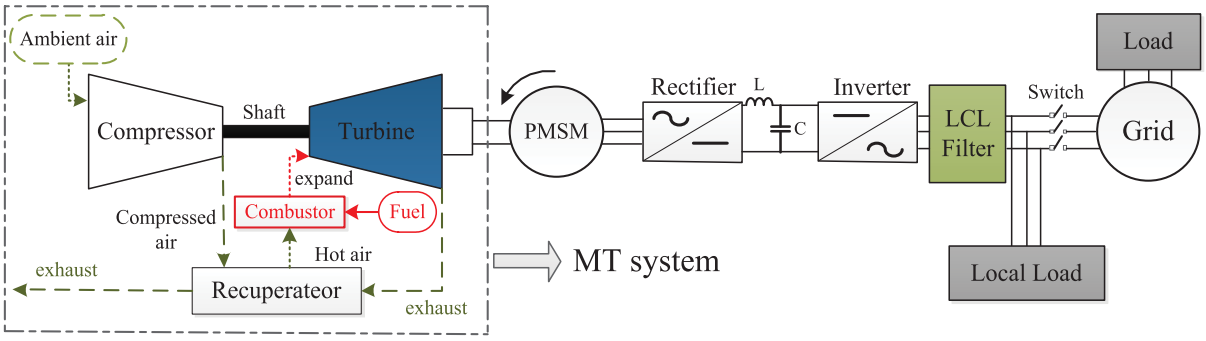

FIGURE 1. The block diagram of the MT system.

fulfill the designated expectations. Thus, advanced nonlinear control approaches should be significantly investigated and supersede the routine PID control [6], [11]. In [12], an adaptive control method is applied to a hybrid power plant system consisting of high-temperature fuel cells and MTs. In [13], by using adaptive backstepping method, a nonlinear turbine steam valve controller has been designed. However, the utilization of backstepping design unavoidably brings heavy calculations on partial differential terms during the recursive design procedure. A novel non-recursive design framework by applying a feedback domination technique has been proposed in [14] for the MT system while the disturbances are intentionally avoided. While, the performances under the above mentioned adaptive control strategies are strongly depended on modeling accuracies. Inevitably, disturbances widely exist in most practical MT systems and may exert adverse effects on the control performance. However, when dealing with the tracking problem of the MT system, few researchers take account of the active attenuation of the mismatched disturbances. Thus, in order to realize high precision tracking control of the MT system, it is imperative to design a disturbance observer with fast dynamics to reduce the adverse effects of disturbances. Then, on the basis of the disturbances being attenuated by the observer, it can go further to design the composite tracking control law.

To this aim, a higher-order sliding mode (HOSM) observer is empolyed in this paper to realize a finite-time system performance recovery. Secondly, inspired by [15]–[17], a non-recursive feedback domination control strategy is utilized to design a tracking control law, which targets at an exact asymptotical tracking objective. In addition, under the proposed non-recursive design manner, a new feature in this paper is the largely reduced design complexity comparing with backstepping based approaches. The main contribution of this paper is that, considering the inaccuracy of the MT system caused by uncertainties and external disturbances, the system can still accomplish exact speed tracking control. By using the Lyapunov stability theory, the rigorous stability analysis is firmly established. To illustrate the high accuracy of HOSM observer and also the efficacy of the proposed composite control strategy, comprehensive simulation comparisons are presented.

The remaining of this paper is organized as follows. In section II, considering the existence of mismatched disturbances, reconstruct Rowen's mathematical model. In section III, a composite controller is integrated by a finite-time disturbance observer (FTDO) and a non-recursive tracking control law. In section IV, regarding the closed-loop system with the disturbance estimation error system as a cascade system, the rigorous stability analysis of the augmented system is provided by using Lyapunov stability theory. In section V, the results of numerical simulation are obtained as an effective demonstration for the proposed approaches. Finally, section VI concludes this paper. In addition, a necessary lemma and notations required for our stability analysis are presented in the Appendix and some other control method design procedures for comparisons are given as well.

II. PROBLEM FORMULATION

In [7] and [18], by omitting the acceleration control loop, the temperature control loop and restructuring system in per-unit values, a simplified nominal mathematical model of the MT system can be presented in the following form

$$\begin{cases} \dot{x}_1 = 1.3/Jx_2 - 1/(2J)x_1 + (0.201 - T_e)/J, \\ \dot{x}_2 = 1/T_{CD}x_3 - 1/T_{CD}x_2, \\ \dot{x}_3 = K_a/T_a x_4 - 1/T_a x_3, \\ \dot{x}_4 = (ck_f/a) \cdot x_1 u - b/a x_4 + ck_l/a, \\ y = x_1, \end{cases} \tag{1}$$

where x_1, x_2, x_3, x_4 and u represent the MT speed, the turbine torque, the fuel flow, the valve position and fuel instruction signal respectively. All the corresponding practical meanings of involved parameters are introduced in Table 1. The main objective of the system is to find an exact tracking control law of a given reference signal depicted as y_r.

However, since model (1) only represents a nominal model of the MT system, whereas the inevitable system uncertainties, external disturbances are not accounted into the modeling. From a practical point of view, model (1) can be

TABLE 1. The involved parameters of the MT model.

Parameters	*Description*
a, b, c	Valve position parameters
K_a, T_a	Fuel actuator parameters
T_{CD}	Discharge lag time constant
J	Inertia of rotor and load
T_e	The electromagnetic torque
k_l	Minimum load
k_f	Maximum fuel demand

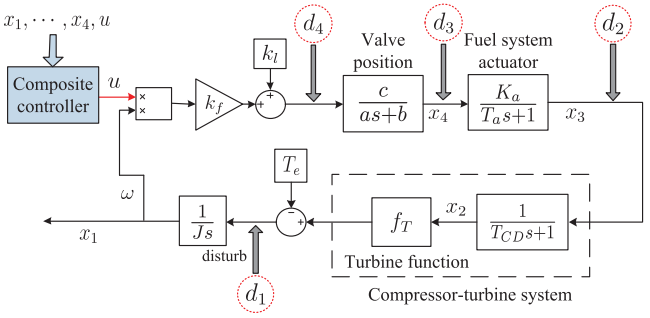

FIGURE 2. The simplified MT system model.

modified to represent a much more general case by taking into the consideration of mismatched lumped disturbances. The lumped disturbance is comprised of system uncertainties and external disturbances. Thus, the following system, as shown in Fig. 2, is considered throughout this paper

$$\begin{cases} \dot{x}_i = g_i x_{i+1} + f_i(x_i) + d_i, & i \in \mathbb{N}_{1:3}, \\ \dot{x}_4 = g_4(y)u + f_4(x_4) + d_4, \\ y = x_1, \end{cases} \tag{2}$$

where $g_1 = 1.3/J$, $g_2 = 1/T_{CD}$, $g_3 = K_a/T_a$, $g_4(y) = ck_f/ax_1$, $f_1 = -1/(2J)x_1 + (0.201 - T_e)/J$, $f_2 = -1/T_{CD}x_2$, $f_3 = -1/T_a x_3$, $f_4 = -b/ax_4 + ck_l/a$, and lumped disturbance terms $d_i = \Delta\theta_i + d_{exi}$, $i \in \mathbb{N}_{1:4}$, $\Delta\theta_i$, d_{exi} represent system internal uncertainties and the external disturbances respectively. In Fig. 2, turbine function $f_T = 1.3(x_2 - 0.23) + 0.5(1 - \omega)$. To proceed, the following assumption, which is highly practical in physical senses, is required for rigorous stability analysis.

Assumption 1: The lummped disturbances $d_i(t)$ in (2) satisfy $d_i \in \mathcal{C}^{4-i}$ and $\max_{i\in\mathbb{N}_{1:4}, j\in\mathbb{N}_{0:4-i}} \left|\frac{\partial^{(j)} d_i(t)}{\partial t^{(j)}}\right| \le \gamma_d^+$, where γ_d^+ is a positive constant.

III. COMPOSITE CONTROLLER CONSTRUCTION

In this section, a composite controller is designed for exact tracking realization rather than a practical control objective. An active disturbance estimation process and an effective tracking control law based on the non-recursive design framework are both essential for the composite controller construction. The proposed composite control method is depicted in Fig. 3.

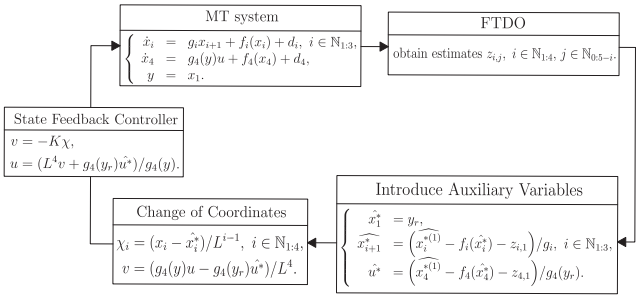

FIGURE 3. The block diagram of the proposed composite control method.

A. FINITE-TIME DISTURBANCE OBSERVER DESIGN

In this subsection, a finite-time performance recovery of the MT system will be achieved by utilizing the following HOSM observer [19]

$$\begin{aligned} \dot{z}_{i,0} &= \hbar_{i,0} + g_i x_{i+1} + f_i(x_i), \quad i \in \mathbb{N}_{1:3}, \\ \hbar_{i,0} &= -\lambda_{i,0}\ell_i^{\alpha_{i,0}} \lfloor z_{i,0} - x_i \rceil^{1-\alpha_{i,0}} + z_{i,1}, \\ \dot{z}_{i,k} &= \hbar_{i,k}, \quad k \in \mathbb{N}_{1:5-i}, \\ \hbar_{i,j} &= -\lambda_{i,j}\ell_i^{\alpha_{i,j}} \lfloor z_{i,j} - \hbar_{i,j-1} \rceil^{1-\alpha_{i,j}} + z_{i,j+1},\ j \in \mathbb{N}_{1:4-i}, \\ \hbar_{i,5-i} &= -\lambda_{i,5-i}\ell_i^{\alpha_{i,5-i}} \lfloor z_{i,5-i} - \hbar_{i,4-i} \rceil^{1-\alpha_{i,5-i}}, \\ \dot{z}_{4,0} &= \hbar_{4,0} + g_4(y)u + f_4(x_4), \\ \hbar_{4,0} &= -\lambda_{4,0}\ell_4^{\alpha_{4,0}} \lfloor z_{4,0} - x_4 \rceil^{1-\alpha_{4,0}} + z_{4,1}, \\ \dot{z}_{4,1} &= \hbar_{4,1} = -\lambda_{4,1}\ell_4^{\alpha_{4,1}} \lfloor z_{4,1} - \hbar_{4,0} \rceil^{1-\alpha_{4,1}}, \end{aligned} \tag{3}$$

where $\alpha_{i,j} = \frac{1}{6-i-j}$, $\lambda_{i,j} \in \mathbb{R}_+$, $\ell_i \in \mathbb{R}_+$ $(i \in \mathbb{N}_{1:4}, j \in \mathbb{N}_{0:5-i})$ are observer parameters to be designed, $z_{i,0} = \hat{x}_i$, $z_{i,j} = \widehat{d_i^{(j-1)}}$. Denote $\hat{x}_i$, $\widehat{d_i^{(j-1)}}$ as the estimates of x_i, $d_i^{(j-1)}$, respectively.

Defining the error of observer as $e_{i,0} = \hat{x}_i - x_i$ and $e_{i,j} = \widehat{d_i^{(j-1)}} - d_i^{(j-1)}$, the error dynamics gives

$$\begin{cases} \dot{e}_{i,0} = -\lambda_{i,0}\ell_i^{\alpha_{i,0}} \lfloor e_{i,0} \rceil^{1-\alpha_{i,0}} + e_{i,1}, \\ \dot{e}_{i,j} = -\lambda_{i,j}\ell_i^{\alpha_{i,j}} \lfloor e_{i,j} - \dot{e}_{i,j-1} \rceil^{1-\alpha_{i,j}} + e_{i,j+1}, \\ \dot{e}_{i,5-i} \in -\lambda_{i,5-i}\ell_i^{\alpha_{i,5-i}} \lfloor e_{i,5-i} \\ \quad -\dot{e}_{i,4-i} \rceil^{1-\alpha_{i,5-i}} + [-\gamma_d{}^+, \gamma_d{}^+]. \end{cases} \tag{4}$$

It follows from [19] that for any well defined $x(t)$, $\ell_i > \gamma_d{}^+$, the error dynamic system (4) will converge to zero after a finite time transient process, that is, there exists a time instant t_f such that $e_{i,j} = 0$, $t > t_f$, $i \in \mathbb{N}_{1:4}$, $j \in \mathbb{N}_{0:5-i}$.

Owing to the FTDO (3), the MT system (2) with mismatched disturbances is provided with the favorable disturbance rejection capability, which facilitates the subsequent exact tracking control law design.

B. EXACT TRACKING CONTROL LAW DESIGN

To clearly delineate the control law design, the designing procedure would be divided into the following two steps.

Step 1: In this step, a change of coordinates is accomplished. A series of auxiliary variables $u^*, x_i^*, i \in \mathbb{N}_{1:4}$, which

are prepared for the coordinates change, are defined by

$$\begin{aligned} x_1^* &= y_r, \\ x_i^* &= \left(x_{i-1}^{*(1)} - f_{i-1}(x_{i-1}^*) - d_{i-1}\right)/g_{i-1}, \quad i \in \mathbb{N}_{2:4}, \\ u^* &= \left(x_4^{*(1)} - f_4(x_4^*) - d_4\right)/g_4(y_r). \end{aligned} \tag{5}$$

Note that (5) is unachievable owing to the fact that disturbance term $d_i^{(j)}$ is unknown. However, with the help of the disturbance observer (3), it brings new auxiliary variables $\widehat{x_i^{*(k)}}$ by merely replacing $d_i^{(j)}$ in (5) with their corresponding estimations $z_{i,j+1}$, $i \in \mathbb{N}_{1:4}$, $j \in \mathbb{N}_{0:4-i}$, $k \in \mathbb{N}_{0:5-i}$. New auxiliary variables can be written as follows

$$\begin{aligned} \hat{x_1^*} &= x_1^* = y_r, \\ \widehat{x_{i+1}^*}(t, \bar{y}_{r,i+1}, \bar{z}_{i+1}) &= \left(\widehat{x_i^{*(1)}} - f_i(\hat{x_i^*}) - z_{i,1}\right)/g_i, \quad i \in \mathbb{N}_{1:3}, \\ \hat{u^*}(t, \bar{y}_{r,5}, \bar{z}_5) &= \left(\widehat{x_4^{*(1)}} - f_4(\hat{x_4^*}) - z_{4,1}\right)/g_4(y_r), \end{aligned} \tag{6}$$

with $\bar{y}_{r,i+1} = (y_r, \cdots, y_r^{(i)})^T, \bar{z}_{i+1} = (z_{1,1}, \cdots, z_{1,i}, \cdots, z_{i,1})^T$, e.g., $\bar{y}_{r,5} = (y_r, \cdots, y_r^{(4)})^T, \bar{z}_5 = (z_{1,1}, \cdots, z_{1,4}, z_{2,1}, \cdots, z_{2,3}, z_{3,1}, z_{3,2}, z_{4,1})^T$, $\widehat{x_2^{*(1)}}(t, y_r^{(1)}, y_r^{(2)}, z_{1,2}) = (y_r^{(2)} + 1/(2J)y_r^{(1)} - (0.201 - T_e)/J - z_{1,2})/g_1$, $\widehat{x_4^{*(1)}} = \widehat{x_4^{*(1)}}(t, y_r^{(1)}, \cdots, y_r^{(4)}, z_{1,2}, z_{1,3}, z_{1,4}, z_{2,2}, z_{2,3}, z_{3,2})$.

Now it is able to define a change of coordinates by introducing a scaling gain $L \geq 1$ as the following form

$$\begin{aligned} \chi_i &= (x_i - \hat{x_i^*})/L^{i-1}, \quad i \in \mathbb{N}_{1:4}, \\ v &= (g_4(y)u - g_4(y_r)\hat{u^*})/L^4. \end{aligned} \tag{7}$$

Then system (2) is equivalent to the following χ-dynamic system,

$$\begin{cases} \dot{\chi}_i = Lg_i\chi_{i+1} + (f_i(x_i) - f_i(\hat{x_i^*}) - e_{i,1} + \widehat{x_i^{*(1)}} - \hat{x_i^*}^{(1)})/L^{i-1}, \\ i \in \mathbb{N}_{1:3}, \\ \dot{\chi}_4 = Lv + (f_4(x_4) - f_4(\hat{x_4^*}) - e_{4,1} + \widehat{x_4^{*(1)}} - \hat{x_4^*}^{(1)})/L^3. \end{cases} \tag{8}$$

Through the aforementioned steps, the initial tracking speed trajectory objective evolves into a stabilization objective, which aims to achieve the stability of the χ-dynamic system (8).

Step II: In this step, a state feedback tracking control law v for system (8) is formulated by

$$v = -K\chi, \tag{9}$$

where $K = (k_1, k_2, k_3, k_4)$ is the coefficient vector of a Hurwitz polynomial $s^4 + k_4 s^3 + k_3 s^2 + k_2 s^1 + k_1$. Combining with (7)-(9), the control input u for the original system (2) should be expressed as

$$u(t) = (L^4 v + g_4(y_r)\hat{u^*})/g_4(y). \tag{10}$$

Before starting the rigorous stability analysis, the above closed-loop system (8)-(9) should be firstly reorganized into the following compact form

$$\dot{\chi} = L(A\chi + Bv) + \Phi + \Psi, \tag{11}$$

where

$$\chi = \begin{bmatrix} \chi_1 \\ \chi_2 \\ \chi_3 \\ \chi_4 \end{bmatrix}, \quad A = \begin{bmatrix} 0 & g_1 & 0 & 0 \\ 0 & 0 & g_2 & 0 \\ 0 & 0 & 0 & g_3 \\ 0 & 0 & 0 & 0 \end{bmatrix}, \; B = \begin{bmatrix} 0 \\ 0 \\ 0 \\ 1 \end{bmatrix},$$

$$\Phi = \left[\{(f_i(x_i) - f_i(\hat{x_i^*}))/L^{i-1}\}_{i \in \mathbb{N}_{1:4},\ 4\times 1}\right],$$

$$\Psi = \left[\{(-e_{i,1} + \widehat{x_i^{*(1)}} - \hat{x_i^*}^{(1)})/L^{i-1}\}_{i \in \mathbb{N}_{1:4},\ 4\times 1}\right].$$

IV. RIGOROUS STABILITY ANALYSIS

The main theorem of this paper is first given as follows.

Theorem 1: Consider the closed-loop system consisting of the MT system (2) satisfying Assumptions 1, the proposed control law (10) and disturbance error system (4). The following statements hold.

i) All the signals in the closed-loop system are uniformly bounded.

ii) The output y will asymptotically track the time-varying signal y_r.

Proof: The following stability proof can be divided into two parts according to different time intervals. The first step is to prove that all the states of the system will not escape to infinity for $t \in [0, t_f)$. With all system states being ensured to be bounded and derivatives of disturbances being exactly estimated at t_f, the second step is to verify the asymptotically stability of the closed-loop system (9)-(11) for $t \in [t_f, +\infty)$.

Part I: In the time interval $[0, t_f)$, errors of disturbances $e_{i,j}$ cannot converge to zero instantly. Thus, the system in this time interval is expressed as (11) with $\Psi \neq 0$. Inspired by [20], in order to ensure the system states will not escape to infinite in $[0, t_f)$, a bounded function consisting of all states of system (11) is designed as follows

$$B(x, z) = \frac{1}{2}\left(\sum_{i=1}^{4}(x_i^2 + z_{i,0}^2) + \bar{z}_5^T\bar{z}_5\right),$$

where $\bar{z}_5 = (z_{1,1}, \cdots, z_{1,4}, z_{2,1} \cdots z_{2,3}, z_{3,1}, z_{3,2}, z_{4,1})^T$.

Taking the first derivative of $B(x, z)$ gives

$$\begin{aligned} \dot{B}(x, z) &= \sum_{i=1}^{4}(x_i\dot{x}_i + z_{i,0}\dot{z}_{i,0}) + \bar{z}_5^T\dot{\bar{z}}_5 \\ &= \sum_{i=1}^{3} x_i(g_i x_{i+1} + f_i(x_i) + d_i) \\ &\quad + x_4(g_4(y)u + f_4(x_4) + d_4) \\ &\quad + \sum_{i=1}^{3} z_{i,0}\left(\hbar_{i,0} + g_i x_{i+1} + f_i(x_i)\right) \\ &\quad + z_{4,0}\left(\hbar_{4,0} + g_4(y)u + f_4(x_4)\right) + \sum_{i=1}^{4} z_{i,1}\hbar_{i,1} \\ &\quad + \sum_{i=1}^{3} z_{i,2}\hbar_{i,2} + \sum_{i=1}^{2} z_{i,3}\hbar_{i,3} + z_{1,4}\hbar_{1,4}. \end{aligned}$$

By using Lemma 1, note that

$$\begin{aligned}
z_{i,0}\hbar_{i,0} &= z_{i,0}(-\lambda_{i,0}\ell_i^{\frac{1}{6-i}}\lfloor z_{i,0}-x_i\rceil^{\frac{5-i}{6-i}}+z_{i,1})\\
&\le \lambda_{i,0}\ell_i^{\frac{1}{6-i}}|z_{i,0}|\big(|z_{i,0}|^{\frac{5-i}{6-i}}+|x_i|^{\frac{5-i}{6-i}}\big)\\
&\quad +|z_{i,0}\cdot z_{i,1}|,\quad i\in\mathbb{N}_{1:4};\\
z_{i,1}\hbar_{i,1} &\le \lambda_{i,1}\ell_i^{\frac{1}{5-i}}|z_{i,1}|\cdot\big(|z_{i,1}|^{\frac{4-i}{5-i}}+|\hbar_{i,0}|^{\frac{4-i}{5-i}}\big)+|z_{i,1}\cdot z_{i,2}|\\
&\le \lambda_{i,1}\ell_i^{\frac{1}{5-i}}|z_{i,1}|^{\frac{9-2i}{5-i}}+\lambda_{i,1}\ell_i^{\frac{1}{5-i}}|z_{i,1}|\\
&\quad\cdot\Big(\lambda_{i,0}^{\frac{4-i}{5-i}}\ell_i^{\frac{4-i}{(5-i)(6-i)}}\big(|z_{i,0}|^{\frac{4-i}{6-i}}+|x_i|^{\frac{4-i}{6-i}}\big)+|z_{i,1}|^{\frac{4-i}{5-i}}\Big)\\
&\quad +|z_{i,1}\cdot z_{i,2}|\\
&\le 2\lambda_{i,1}\ell_i^{\frac{1}{5-i}}|z_{i,1}|^{\frac{9-2i}{5-i}}+\lambda_{i,0}^{\frac{4-i}{5-i}}\lambda_{i,1}\ell_i^{\frac{2}{6-i}}|z_{i,1}|\\
&\quad\cdot\big(|z_{i,0}|^{\frac{4-i}{6-i}}+|x_i|^{\frac{4-i}{6-i}}\big)+|z_{i,1}\cdot z_{i,2}|,\ i\in\mathbb{N}_{1:3};\\
z_{i,2}\hbar_{i,2} &\le 2\lambda_{i,2}\ell_i^{\frac{1}{4-i}}|z_{i,2}|^{\frac{7-2i}{4-i}}+2\lambda_{i,1}^{\frac{3-i}{4-i}}\lambda_{i,2}\ell_i^{\frac{2}{5-i}}|z_{i,1}|^{\frac{3-i}{5-i}}|z_{i,2}|\\
&\quad+\lambda_{i,0}^{\frac{3-i}{5-i}}\lambda_{i,1}^{\frac{3-i}{4-i}}\lambda_{i,2}\ell_i^{\frac{3}{6-i}}|z_{i,2}|\big(|z_{i,0}|^{\frac{3-i}{6-i}}+|x_i|^{\frac{3-i}{6-i}}\big)\\
&\quad+|z_{i,2}\cdot z_{i,3}|,\ i\in\mathbb{N}_{1:2};\\
z_{1,3}\hbar_{1,3} &\le 2\lambda_{1,3}\ell_1^{\frac{1}{2}}|z_{1,3}|^{\frac{3}{2}}+2\lambda_{1,2}^{\frac{1}{2}}\lambda_{1,3}\ell_1^{\frac{2}{3}}|x_{1,2}|^{\frac{1}{3}}|z_{1,3}|\\
&\quad+2\lambda_{1,1}^{\frac{1}{3}}\lambda_{1,2}^{\frac{1}{2}}\lambda_{1,3}\ell_1^{\frac{3}{4}}|z_{1,1}|^{\frac{1}{4}}\cdot|z_{1,3}|\\
&\quad+\lambda_{1,0}^{\frac{1}{4}}\lambda_{1,1}^{\frac{1}{3}}\lambda_{1,2}^{\frac{1}{2}}\lambda_{1,3}\ell_1^{\frac{4}{5}}|z_{1,3}|\cdot\big(|z_{1,0}|^{\frac{1}{5}}+|x_1|^{\frac{1}{5}}\big)\\
&\quad+|z_{1,3}\cdot z_{1,4}|.
\end{aligned}$$

The following relations also hold

$$z_{5-i,i}\hbar_{5-i,i}\le\lambda_{5-i,i}\ell_{5-i}z_{5-i,i},\quad i\in\mathbb{N}_{1:4}.$$

On the one hand, let $\eta=\sqrt{\sum_{i=1}^{4}(x_i^2+z_{i,0}^2)+\bar{z}_5^T\bar{z}_5}$. If $\eta>1$, it can be easily obtained that $|x_i|\le\eta\le\eta^2$, $z_{i,j}\le\eta\le\eta^2$, $x_ix_k\le\eta^2$, $x_kz_{i,j}\le\frac{\eta^2}{2}$, where $i\in\mathbb{N}_{1:4}$, $j\in\mathbb{N}_{0:5-i}$, $k\in\mathbb{N}_{1:4}$. Hence

$$\begin{aligned}
x_1\dot{x}_1 &\le \Big(\frac{g_1}{2}-\frac{1}{2J}+\frac{0.201-T_e}{J}+\gamma_d^+\Big)\eta^2,\\
x_2\dot{x}_2 &\le \Big(\frac{g_2}{2}-\frac{1}{T_{CD}}+\gamma_d^+\Big)\eta^2,\\
x_3\dot{x}_3 &\le \Big(\frac{g_3}{2}-\frac{1}{T_a}+\gamma_d^+\Big)\eta^2.
\end{aligned}$$

Considering that the reference signal y_r and its higher order derivatives are bounded, from (6), one can conclude that there exists a positive constant $\bar{\kappa}$ to render $g_4(y_r)\hat{u^*}\le\bar{\kappa}$. Further, with the relationship $g_4(y_r)\hat{u^*}x_4\le\bar{\kappa}\eta^2$ being valid, the following inequality holds

$$\begin{aligned}
x_4\dot{x}_4 &= x_4\Big(L^4K\chi+g_4(y_r)\hat{u^*}+f_4(x_4)+d_4\Big)\\
&\le \Big(\frac{3}{2}L^4(k_1+\cdots+k_4)+\bar{\kappa}+\frac{ck_l-b}{a}+\gamma_d^+\Big)\eta^2.
\end{aligned}$$

Thus

$$\begin{aligned}
&\dot{B}(x,z)\\
&\le \Big(\frac{g_1+g_2+g_3}{2}-\frac{1}{2J}+\frac{0.201-T_e}{J}-\frac{1}{T_{CD}}\\
&\quad-\frac{1}{T_a}+\frac{3}{2}L^4(k_1+\cdots+k_4)+\bar{\kappa}+\frac{ck_l-b}{a}+4\gamma_d^+\Big)\eta^2\\
&\quad+\Big(\sum_{i=1}^{4}2\lambda_{i,0}\ell_i^{\frac{1}{6-i}}\Big)\eta^2+2\eta^2\\
&\quad+\Big(\sum_{i=1}^{3}2\lambda_{i,1}\ell_i^{\frac{1}{5-i}}+2\lambda_{i,0}^{\frac{4-i}{5-i}}\lambda_{i,1}\ell_i^{\frac{2}{6-i}}\Big)\eta^2+\frac{3}{2}\eta^2\\
&\quad+\Big(\sum_{i=1}^{2}2\lambda_{i,2}\ell_i^{\frac{1}{4-i}}+2\lambda_{i,1}^{\frac{3-i}{4-i}}\lambda_{i,2}\ell_i^{\frac{2}{5-i}}+2\lambda_{i,0}^{\frac{3-i}{5-i}}\lambda_{i,1}^{\frac{3-i}{4-i}}\lambda_{i,2}\ell_i^{\frac{3}{6-i}}\Big)\eta^2\\
&\quad+\eta^2+\sum_{i=1}^{4}\lambda_{5-i,i}\ell_{5-i}\eta^2\\
&= 2HB(x,z),
\end{aligned}\tag{12}$$

where $H=\frac{g_1+g_2+g_3}{2}-\frac{1}{2J}+\frac{0.201-T_e}{J}-\frac{1}{T_{CD}}-\frac{1}{T_a}+\frac{3}{2}L^4(k_1+\cdots+k_4)+\bar{\kappa}+\frac{ck_l-b}{a}+4\gamma_d^+\sum_{i=1}^{4}2\lambda_{i,0}\ell_i^{\frac{1}{6-i}}+\cdots+\sum_{i=1}^{2}(2\lambda_{i,2}\ell_i^{\frac{1}{4-i}}+2\lambda_{i,1}^{\frac{3-i}{4-i}}\lambda_{i,2}\ell_i^{\frac{2}{5-i}}+2\lambda_{i,0}^{\frac{3-i}{5-i}}\lambda_{i,1}^{\frac{3-i}{4-i}}\lambda_{i,2}\ell_i^{\frac{3}{6-i}})+1+\sum_{i=1}^{4}\lambda_{5-i,i}\ell_{5-i}$ and it is a constant. From the inequality (12), it is easy to obtain that $B(x,z)\le B(x(0),z(0))e^{2Ht}$.

On the other hand, if $\eta\le1$, there exists a positive constant $\tilde{L}$ satisfying $\dot{B}(x,z)\le\tilde{L}\le HB(x,z)+\tilde{L}$. Solving the above inequality, it reaches $B(x,z)\le\Big((HB(x(0),z(0))+\tilde{L})e^{Ht}-\tilde{L}\Big)/H$. This suggests that $B(x,z)$ is bounded and the system states, including x and z, will not diverge to infinite within t_f.

Then according to the expression of $\hat{x_i^*}$ in (6), $i\in\mathbb{N}_{1:4}$, it is undoubted that $\hat{x_i^*}$ are bounded, and consequently χ_i would also be bounded in $[0,t_f)$.

Part II: Considering that $t\in[t_f,+\infty)$, that is $e_{i,j}=0$, system (11) can be rewritten in the following from

$$\begin{cases}\dot{\chi}=L(A\chi+Bv)+\Phi,\\ y=C\chi+y_r.\end{cases}\tag{13}$$

Construct a positive definite Lyapunov function as the following form

$$V=\chi^TP\chi,\tag{14}$$

where P is a positive definite, symmetrical matrix satisfying

$$(A-BK)^TP+P(A-BK)=-I.$$

Taking the derivative of (14) along the system (10) (13), it has

$$\begin{aligned}
\dot{V} &= \frac{\partial V}{\partial\chi^T}\Big(L(A-BK)\chi+\Phi\Big)\\
&= \frac{\partial V}{\partial\chi^T}L(A-BK)\chi+\sum_{i=1}^{4}\frac{\partial V}{\partial\chi_i}(f_i(x_i)-f_i(\hat{x_i^*})/L^{i-1})\\
&\le -L\|\chi\|_2^2+\sum_{i=1}^{4}\frac{\partial V}{\partial\chi_i}(f_i(x_i)-f_i(\hat{x_i^*})/L^{i-1}).
\end{aligned}\tag{15}$$

TABLE 2. The values of MT model parameters.

Parameter	a	b	c	K_a	T_a	T_{CD}	J	T_e	k_l	k_f
Value	0.05	1	1	1	0.4	0.2(s)	$8\times10^{-4}(Kg\cdot m^2)$	0.2	0.23	0.77

From system (2), $f_i(\cdot)$ satisfies the global Lipschitz continuous condition, i.e., $|f_i(x_i) - f_i(\hat{x}_i^*)| \le l_i|\chi_i|$, for a constant $l_i \in \mathbb{R}_+$. In this sense, inequality (15) can be written

$$\begin{aligned}&\sum_{i=1}^{4}\frac{\partial V}{\partial \chi_i}(f_i(x_i)-f_i(\hat{x}_i^*)/L^{i-1})\\ &\le \sum_{i=1}^{4}\frac{\partial V}{\partial \chi_i}|\chi_i|\cdot(l_i/L^{i-1})\\ &\le \max_{i\in\mathbb{N}_{1:4}}\{l_i\}\sum_{i=1}^{4}\frac{\partial V}{\partial \chi_i}|\chi_i| \le \alpha\|\chi\|_2^2,\end{aligned} \tag{16}$$

where $\alpha \in \mathbb{R}_+$ is a constant which is independent of L. Combining inequalities (15) and (16), it can be obtained that

$$\dot{V} \le -(L-\alpha)\|\chi\|_2^2. \tag{17}$$

If the scaling gain L is set to be sufficiently large such that $L > \alpha$, the inequality (17) further reduces to $\dot{V} \le 0$, thus reaching the conclusion that the system (13) is asymptotically stable for $t \in [t_f, +\infty)$.

Concluded from the above reasoning, the closed-loop system consisting of χ-dynamic system (8), disturbance error system (4) and exact tracking control law (10) is asymptotically stable. This completes the proof of Theorem 1. ■

Remark 1: The parameters $\lambda_{i,j}$, ℓ_i of the FTDO with $i \in \mathbb{N}_{1:4}$, $j \in \mathbb{N}_{0:4-i}$ can be chosen by repeated trials. The values of ℓ_i are tuned to adjust the convergence rate of finite-time differentiator. Specifically, the larger ℓ_i is, the faster convergence rate of the differentiator is, and vice versa [20].

Remark 2: For fair comparisons, the explicit backstepping design procedure for the MT system without the presence of disturbances is also provided in the Appendix. It is straightforward to recognize that a plethora of partial differential terms are induced in the design process. Differently, the proposed non-recursive design framework could essentially avoid the calculation of partial differential terms, which considerably mitigates computational burdens of the control law.

V. NUMERICAL SIMULATIONS

Considering the practical mathematical MT model (2) as the simulation target, related parameters are shown in Table 2. We select sinusoidal waves as unknown disturbances to verify the effectiveness of the FTDO, which are

$$\begin{aligned}d_1 &= 0.2\sin(t), \quad d_2 = 0.2\sin(t+\pi/2)+0.2,\\ d_3 &= 0.2\sin(2t+\pi/4), \quad d_4 = -0.1+0.2\sin(0.5t).\end{aligned}$$

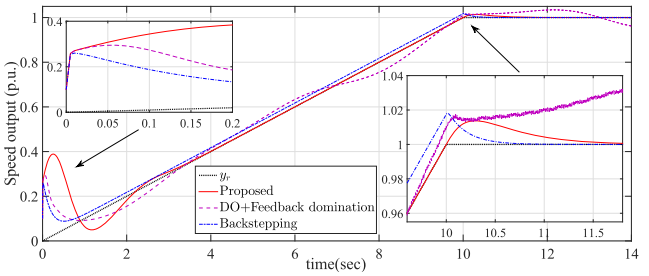

FIGURE 4. The speed tracking performance.

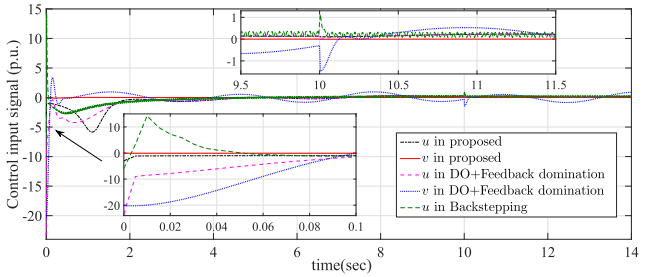

FIGURE 5. Time histories of the control inputs.

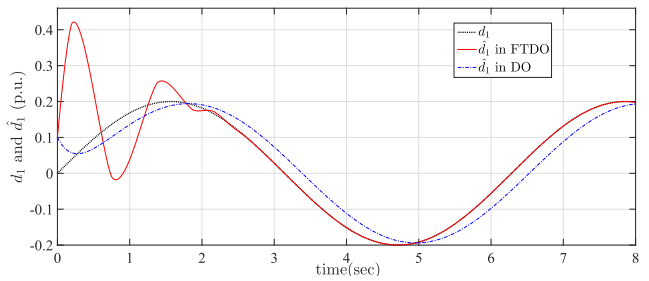

FIGURE 6. Response curves of the estimates of d_1.

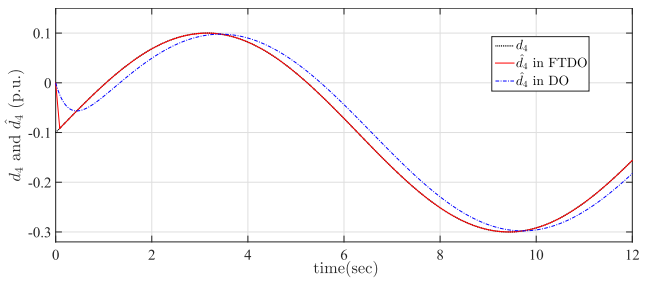

FIGURE 7. Response curves of the estimates of d_4.

The desired reference speed signal y_r is set as

$$y_r = \begin{cases}0.1t & (0 \le t \le 10),\\ 1 & (t > 10),\end{cases}$$

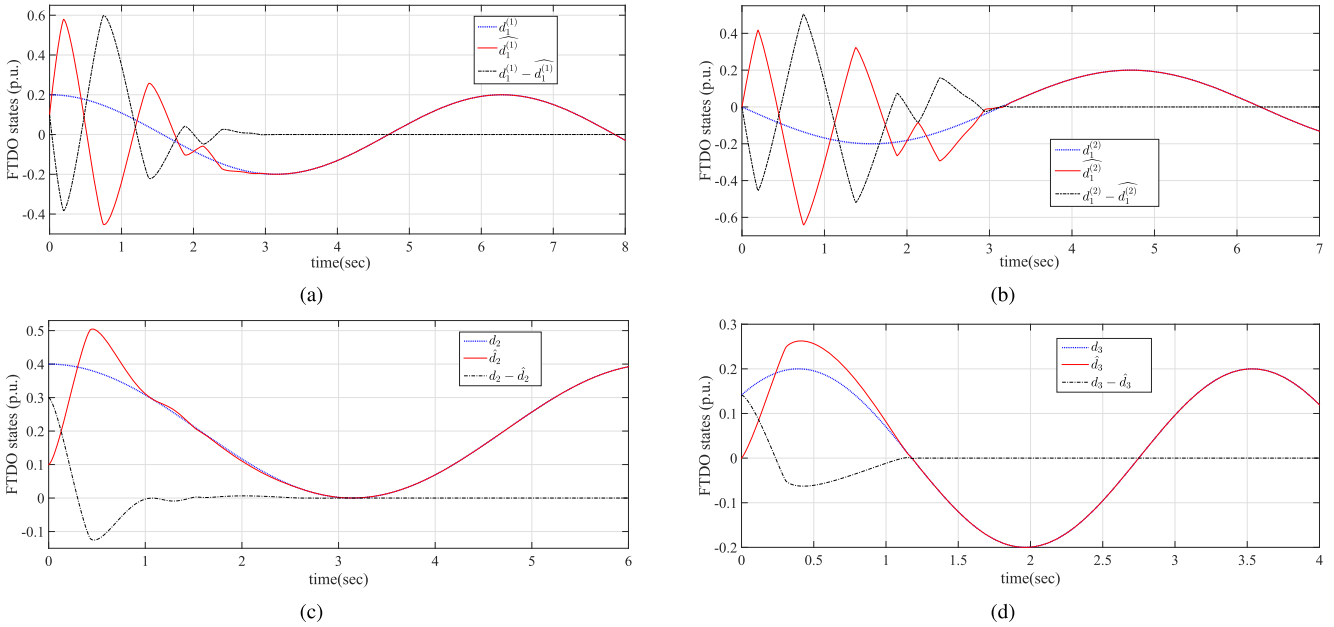

FIGURE 8. The FTDO performance: (a) $d_1^{(1)}$ and $\widehat{d_1^{(1)}}$; (b) $d_1^{(2)}$ and $\widehat{d_1^{(2)}}$; (c) d_2 and $\hat{d}_2$; (d) d_3 and $\hat{d}_3$.

which is a continuous piecewise function, including a uniform acceleration starting stage and a constant speed operation stage.

To conduct the simulation, all the involved parameters are selected as: $\lambda_{1,0} = 4$, $\lambda_{1,1} = 3.9$, $\lambda_{1,2} = 1.8$, $\lambda_{1,3} = 1.2$, $\lambda_{1,4} = 0.9$, $\lambda_{2,0} = 2$, $\lambda_{2,1} = 3.1$, $\lambda_{2,2} = 0.5$, $\lambda_{2,3} = 0.5$, $\lambda_{3,0} = 1.9$, $\lambda_{3,1} = 0.7$, $\lambda_{3,2} = 0.8$, $\lambda_{4,0} = 2.3$, $\lambda_{4,1} = 0.9$, $\ell_1 = 1.6$, $\ell_2 = 1.8$, $\ell_3 = 1.3$, $\ell_4 = 1.2$. Also, the coefficient vector of the state feedback control law (9) is $K = (k_1,\ k_2,\ k_3,\ k_4) = (0.1,\ 3,\ 37,\ 1)$, and the eigenvalues of $A - BK$ are $\lambda_{A-BK} = \{-0.463 \pm 7.4987i,\ -0.037 \pm 5.9987i\}$. The value of L is set as 1.1 in the simulation. The initial values to trigger this simulation are given as

$$\begin{aligned}&\Big(x_1(0),\ x_2(0),\ x_3(0),\ x_4(0),\ \hat{x}_1^*(0),\ \hat{x}_2^*(0),\ \hat{x}_3^*(0),\ \hat{x}_4^*(0),\\ &\quad \hat{d}_1(0),\ \hat{d}_2(0),\ \hat{d}_3(0),\ \hat{d}_4(0),\ \widehat{d_1^{(1)}}(0),\ \widehat{d_2^{(1)}}(0),\ \widehat{d_3^{(1)}}(0),\\ &\quad \widehat{d_1^{(2)}}(0),\ \widehat{d_2^{(2)}}(0),\ \widehat{d_1^{(3)}}(0)\Big) = \Big(0.1,\ 0.1,\ 0.1,\ 0.1,\ 0,\\ &\quad 0.1,\ 0.1,\ 0.1,\ 0.1,\ 0.1,\ 0,\ 0,\ 0.1,\ 0,\ 0.2,\ 0,\ 0,\ 0\Big).\end{aligned}$$

In order to show the advantages of the proposed composite controller (FTDO+Feedback domination), the DO (disturbance observer)+Feedback domination and the backstepping methods are employed for comparative studies. The DO and the backstepping design procedures and relevant parameters are expounded in the Appendix.

The response curves of the MT speed are illustrated in Fig. 4, which shows that the steady state performance of the proposed method is superior to other two control methods. In Fig. 4, the response curve of the DO+Feedback domination can only converge to a small neighborhood region of y_r. Additionally, in Fig. 4, there is a relatively fixed deviation between the response curve of the backstepping and the reference speed y_r for $t \in (1,\ 10)$. This deviation can be eliminated by tuning the parameters of the backstepping controller, but it will cause the control input value to be excessively large at the initial instant.

Since the backstepping method does not employ disturbance attenuation process, it is not comparable of the transient time performance between the backstepping method and the proposed method. In Fig. 4, the transient oscillation of the proposed method is a little larger than that of the DO+Feedback domination method. While the transient time performance of the proposed is still fine and limited in a reasonable region, and the response curve of the proposed method converges to y_r faster than that of the DO+Feedback domination method.

The time histories of control inputs are presented in Fig. 5, which shows that the control energies of another two methods are larger than the proposed method for $t \in (0,\ 0.1)$. It increases the practical control difficulty for high control energy consumption at the beginning.

By Fig. 8, it is observed that the different time derivatives of disturbances can be exactly estimated within a finite time by the proposed FTDO. It can be concluded from Figs. 6-7 that, compared with FTDO, the linear DO fails to realize the exact estimation of the respective disturbances. Overall, the proposed method avoids an over large input energy of the beginning phase. Meanwhile, it can quickly converge to the reference signal and realize the exact tracking control objective even with the presence of mismatched disturbances.

VI. CONCLUSIONS

In this paper, the problem of exact tracking control for the practical MT system with mismatched disturbances has been investigated. A novel composite controller is proposed by

incorporating a FTDO and the non-recursive tracking design strategy. Owing to the FTDO, the disturbances can be completely offset. Then a feedback domination approach is proposed to guarantee the asymptotic stability of the closed-loop system. Finally, simulation results show that the designed composite controller can realize the exact tracking for the MT speed. Necessary comparisons also reveal the advantages of the proposed controller over the existing methods.

APPENDIX

A. A USEFUL LEMMA AND NOTIONS

A useful lemma is stated as follows for the convenience of readers.

Lemma 1: [22] The inequality $(|x_1|+\cdots+|x_n|)^p \le |x_1|^p+\cdots+|x_n|^p$ holds for $x_i \in \mathbb{R}$, $i \in \mathbb{N}_{1:n}$, where $p \in (0, 1]$.

For the briefness of expressions in this paper, the following notations are provided.

The symbol $\mathcal{C}^i$ denotes the set ratio of all differentiable functions whose first i-th time derivatives are continuous. A continuous function $\lfloor\cdot\rceil^\alpha$ is defined by $\lfloor\cdot\rceil^\alpha = \text{sign}(\cdot)|\cdot|^\alpha$. For integers j and i satisfying $0 \le j \le i$, denote $\mathbb{N}_{j:i}$ as $\{j, j+1, \cdots, i\}$. $\mathbb{R}_+$ denotes positive real number. $\|x\|_p = (\sum_{i=1}^n |x_i|^p)^{1/p}$ denotes a conventional L_p norm.

B. DO DESIGN

A disturbance observer [23], [24] used in numerical simulation section is designed as follows

$$\begin{cases} \hat{d}_i = n_i(x_i - p_i), \\ \dot{p}_i = g_i x_{i+1} + f_i(x_i) + \hat{d}_i, \quad i \in \mathbb{N}_{1:3}, \\ \hat{d}_4 = n_4(x_4 - p_4), \\ \dot{p}_4 = g_4(y)u + f_4(x_4) + \hat{d}_4, \end{cases}$$

where $n_i > 0$, $i \in \mathbb{N}_{1:4}$, are design parameters. In the numerical simulation, we set $(n_1,\ n_2,\ n_3,\ n_4) = (6,\ 3,\ 3,\ 3.4)$.

C. BACKSTEPPING DESIGN

Consider the MT system (2) without the presence of disturbances. The recursive backstepping design procedure is shown as the following steps.

Step 1: Choose a Lyapunov function as

$$V_1 = \frac{1}{2}\zeta_1^2,$$

where $\zeta_1 = x_1 - x_1^*$, the virtual control law $x_1^* = y_r$. Taking the derivative of V_1 yields

$$\begin{aligned} \dot{V}_1 &= \zeta_1(g_1 x_2 + f_1(x_1) - y_r^{(1)}), \\ &= \zeta_1\Big(g_1(x_2 - x_2^*) + g_1 x_2^* + f_1(x_1) - y_r^{(1)}\Big). \end{aligned} \tag{18}$$

The virtual control law x_2^* is designed as

$$x_2^* = \frac{1}{g_1}\Big(-\kappa_1\zeta_1 - (f_1(x_1) - y_r^{(1)})\Big), \tag{19}$$

where $\kappa_1 > 0$ is the design parameter. Substituting (19) into (18) yields

$$\dot{V}_1 = -\kappa_1\zeta_1^2 + g_1\zeta_1\zeta_2,$$

where $\zeta_2 = x_2 - x_2^*$.

Step i ($i \in \mathbb{N}_{2:3}$) : Choose a Lyapunov function as

$$V_i = V_{i-1} + \frac{1}{2}\zeta_i^2.$$

The time derivative of V_i is obtained as

$$\begin{aligned} \dot{V}_i = &-\sum_{j=1}^{i-1}\kappa_j\zeta_j^2 + g_{i-1}\zeta_{i-1}\zeta_i + g_i\zeta_i(x_{i+1} - x_{i+1}^*) + g_i\zeta_i x_{i+1}^* \\ &+ \zeta_i f_i(x_i) - \zeta_i\Big(\sum_{j=1}^{i-1}\frac{\partial x_i^*}{\partial x_j}\cdot\frac{dx_j}{dt} + \sum_{j=0}^{i-1}\frac{\partial x_i^*}{\partial y_r^{(j)}}y_r^{(j+1)}\Big). \end{aligned} \tag{20}$$

The virtual control law x_{i+1}^* is designed as

$$\begin{aligned} x_{i+1}^* = \frac{1}{g_i}\Big(&-g_{i-1}\zeta_{i-1} - \kappa_i\zeta_i - f_i(x_i) \\ &+ \sum_{j=1}^{i-1}\frac{\partial x_i^*}{\partial x_j}\cdot\frac{dx_j}{dt} + \sum_{j=0}^{i-1}\frac{\partial x_i^*}{\partial y_r^{(j)}}y_r^{(j+1)}\Big), \end{aligned} \tag{21}$$

where $\kappa_3 > 0$. Substituting (21) into (20) yields

$$\dot{V}_i = -\sum_{j=1}^{i}\kappa_j\zeta_j^2 + g_i\zeta_i\zeta_{i+1},$$

where $\zeta_{i+1} = x_{i+1} - x_{i+1}^*$.

Step 4: Choose a Lyapunov function as

$$V_4 = V_3 + \frac{1}{2}\zeta_4^2.$$

The time derivative of V_4 is obtained as

$$\begin{aligned} \dot{V}_4 = &-\kappa_1\zeta_1^2 - \kappa_2\zeta_2^2 - \kappa_3\zeta_3^2 + g_3\zeta_3\zeta_4 + g_4(y)\zeta_4(u - x_5^*) \\ &+ g_4(y)\zeta_4 x_5^* + \zeta_4 f_4(x_4) \\ &- \zeta_4\Big(\sum_{i=1}^{3}\frac{\partial x_4^*}{\partial x_i}\cdot\frac{dx_i}{dt} + \sum_{i=0}^{3}\frac{\partial x_4^*}{\partial y_r^{(i)}}y_r^{(i+1)}\Big), \end{aligned} \tag{22}$$

where

$$\begin{aligned} &\frac{\partial x_4^*}{\partial x_1} = \frac{1}{g_3}\Big(\frac{g_2}{g_1}\Big(\frac{1}{2J} - \kappa_1\Big) - \frac{1}{2J}\cdot\frac{\partial x_3^*}{\partial x_1} + \kappa_3\frac{\partial x_3^*}{\partial x_1}\Big), \\ &\frac{\partial x_4^*}{\partial x_2} = \frac{1}{g_3}\Big(-g_2 + g_1\frac{\partial x_3^*}{\partial x_1} - \frac{1}{T_{CD}}\cdot\frac{\partial x_3^*}{\partial x_2} + \kappa_3\frac{\partial x_3^*}{\partial x_2}\Big), \\ &\frac{\partial x_4^*}{\partial x_3} = \frac{1}{g_3}\Big(\frac{1}{T_a} + g_2\frac{\partial x_3^*}{\partial x_2} - \kappa_3\Big), \quad \frac{\partial x_4^*}{\partial y_r} = \frac{1}{g_3}\Big(\frac{\kappa_1 g_2}{g_1} + \kappa_3\frac{\partial x_3^*}{\partial y_r}\Big), \\ &\frac{\partial x_4^*}{\partial y_r^{(1)}} = \frac{1}{g_3}\Big(\frac{g_2}{g_1} + \frac{\partial x_3^*}{\partial y_r} + \kappa_3\frac{\partial x_3^*}{\partial y_r^{(1)}}\Big), \\ &\frac{\partial x_4^*}{\partial y_r^{(2)}} = \frac{1}{g_3}\Big(\frac{\partial x_3^*}{\partial y_r^{(1)}} + \kappa_3\frac{\partial x_3^*}{\partial y_r^{(2)}}\Big), \quad \frac{\partial x_4^*}{\partial y_r^{(3)}} = \frac{1}{g_3}\frac{\partial x_3^*}{\partial y_r^{(2)}}. \end{aligned}$$

The virtual control law x_5^* is designed as

$$\begin{aligned} x_5^* = \frac{1}{g_4}\Big(&-g_3\zeta_3 - \kappa_4\zeta_4 - f_4(x_4) \\ &+ \sum_{i=1}^{3}\frac{\partial x_4^*}{\partial x_i}\cdot\frac{dx_i}{dt} + \sum_{i=0}^{3}\frac{\partial x_4^*}{\partial y_r^{(i)}}y_r^{(i+1)}\Big), \end{aligned} \tag{23}$$

where $\kappa_4 > 0$. Substituting (23) into (22) yields

$$\dot{V}_4 = -\kappa_1\zeta_1^2 - \kappa_2\zeta_2^2 - \kappa_3\zeta_3^2 - \kappa_4\zeta_4^2 + g_4(y)\zeta_4\zeta_5,$$

where $\zeta_5 = u - x_5^*$. The actual control input is given by $u = x_5^*$. The backstepping control parameters are given as $(\kappa_1,\ \kappa_2,\ \kappa_3,\ \kappa_4) = (1,\ 4853.477,\ 70,\ 5)$.

REFERENCES

[1] A. Bertani, C. Bossi, F. Fornari, S. Massucco, S. Spelta, and F. Tivegna, "A microturbine generation system for grid connected and islanding operation," in *Proc. Power Syst. Conf. Expo.*, Oct. 2004, pp. 360–365.
[2] S. R. Guda, C. Wang, and M. H. Nehrir, "A simulink-based microturbine model for distributed generation studies," in *Proc. Power Symp.*, Oct. 2005, pp. 269–274.
[3] M. Soliman, M. M. R. Ahmed, and M. Safiuddin, "Modeling of fuel cell/microturbine generation scheme with battery storage," in *Proc. Electr. Power Energy Conf.*, Aug. 2010, pp. 1–6.
[4] R. Lasseter, "Dynamic models for micro-turbines and fuel cells," in *Proc. Power Eng. Soc. Summer Meeting*, Jul. 2001, pp. 761–766.
[5] F. S. Pai and S. J. Huang, "Design and operation of power converter for microturbine powered distributed generator with capacity expansion capability," *IEEE Trans. Energy Convers.*, vol. 23, no. 1, pp. 110–118, Mar. 2008.
[6] T. Yu and J.-P. Tong, "Auto disturbance rejection control of microturbine system," in *Proc. IEEE Power Energy Soc. Gen. Meeting-Convers. Del. Elect. Energy 21st Century*, Jul. 2008, pp. 1–6.
[7] D. N. Gaokar, R. N. Patel, and G. N. Pillai, "Dynamic model of microturbine generation system for grid connected/islanding operation," in *Proc. Int. Conf. Ind. Technol.*, Dec. 2006, pp. 305–310.
[8] X. Xu, H. Jia, H. D. Chiang, D. C. Yu, and D. Wang, "Dynamic modeling and interaction of hybrid natural gas and electricity supply system in microgrid," *IEEE Trans. Power Syst.*, vol. 30, no. 3, pp. 1212–1221, May 2015.
[9] W. I. Rowen, "Simplified mathematical representations of heavy-duty gas turbines," *J. Eng. Power*, vol. 105, no. 4, pp. 865–869, 1983.
[10] A. Rodriguez-Martinez, R. Garduno-Ramirez, and L. G. Vela-Valdes, "PI fuzzy gain-scheduling speed control at startup of a gas-turbine power plant," *IEEE Trans. Energy Convers.*, vol. 26, no. 1, pp. 310–317, Mar. 2011.
[11] S. Jovanovic, B. W. Hogg, and B. Fox, "Intelligent adaptive turbine controller," *IEEE Trans. Energy Convers.*, vol. 10, no. 1, pp. 195–198, Mar. 1995.
[12] F. Jurado and J. R. Saenz, "Adaptive control of a fuel cell-microturbine hybrid power plant," *IEEE Trans. Energy Convers.*, vol. 18, no. 2, pp. 342–347, Jun. 2003.
[13] W. Li, S. Liu, G. Jiang, and G. M. Dimirovski, "Adaptive robust backstepping design for turbine valve controller," in *Proc. 6th World Congr. Intell. Control Automat.*, Jun. 2006, pp. 7439–7443.
[14] X. Xu and C. Zhang, "Realization of finite-time robust speed tracking control for a micro-turbine as a distributed energy resource," in *Proc. IEEE Conf. Ind. Electron. Appl.*, Jun. 2017, pp. 53–58.
[15] C. Zhang, Y. Yan, A. Narayan, and H. Yu, "Practically oriented finite-time control design and implementation: Application to a series elastic actuator," *IEEE Trans. Ind. Electron.*, vol. 65, no. 5, pp. 4166–4176, May 2018.
[16] C. Zhang, Y. Yan, C. Wen, J. Yang, and H. Yu, "A nonsmooth composite control design framework for nonlinear systems with mismatched disturbances: Algorithms and experimental tests," *IEEE Trans. Ind. Electron.*, vol. 65, no. 11, pp. 8828–8839, Nov. 2018.
[17] J. Yang, Z. Ding, S. Li, and C. Zhang, "Continuous finite-time output regulation of nonlinear systems with unmatched time-varying disturbances," *IEEE Control Syst. Lett.*, vol. 2, no. 1, pp. 97–102, Jan. 2018.
[18] A. K. Saha, S. Chowdhury, S. P. Chowdhury, and P. A. Crossley, "Modeling and performance analysis of a microturbine as a distributed energy resource," *IEEE Trans. Energy Convers.*, vol. 24, no. 2, pp. 529–538, Jun. 2009.
[19] A. Levant, "Higher-order sliding modes, differentiation and output-feedback control," *Int. J. Control*, vol. 76, nos. 9–10, pp. 924–941, Jan. 2003.
[20] S. Li, H. Sun, J. Yang, and X. Yu, "Continuous finite-time output regulation for disturbed systems under mismatching condition," *IEEE Trans. Autom. Control*, vol. 60, no. 1, pp. 277–282, Jan. 2015.
[21] X. Tan, X. Su, K. Zhao, and M. Tan, "Robust adaptive backstepping control of micro-turbines," in *Proc. Chin. Control Decis. Conf.*, May 2016, pp. 490–493.
[22] H. Hardy, J. Littlewood, and G. Polya, *Inequalities*. Cambridge, U.K.: Cambridge Univ. Press, 1934, pp. 115–138.
[23] H. Sun, S. Li, J. Yang, and W. X. Zheng, "Global output regulation for strict-feedback nonlinear systems with mismatched nonvanishing disturbances," *Int. J. Robust Nonlinear Control*, vol. 25, no. 15, pp. 2631–2645, 2015.
[24] Q. Xu, C. Zhang, C. Wen, and P. Wang, "A novel composite nonlinear controller for stabilization of constant power load in DC microgrid," *IEEE Trans. Smart Grid*, to be published.

YUGE SUN, photograph and biography not available at the time of publication.

CHUANLIN ZHANG, photograph and biography not available at the time of publication.

HUI CHEN, photograph and biography not available at the time of publication.

PENGFENG LIN, photograph and biography not available at the time of publication.

XINGCHEN XU, photograph and biography not available at the time of publication.